文章编号 1674-2915(2008)01-0085-07

# Electrospinning preparation and oxygen sensing properties of dirhenium(Ⅰ) complex/polymer composite fibers

LIU Yan-hong[1,2], LI Bin[1], CONG Yan[1,2]

(1. *Key Laboratory of Excited State Processes, Changchun Institute of Optics, Fine Mechanics and Physics, Chinese Academy of Sciences, Changchun* 130033, *China*;
2. *Graduate University of Chinese Academy of Sciences, Beijing* 100039, *China*)

**Abstract**: A novel lipophilic dirhenium complex *fac*-[{Re(CO)$_3$(d19-phen)}$_2$(4,4′-bipyridyl)](OTf)$_2$ (denoted as D-Re(I)) (d19-phen = 4,7-dinonadecyl-1,10-phenanthroline and OTf = trifluoromethane-sulfonate) was doped homogeneously in polystyrene (PS) and polymethyl methacrylate (PMMA) fibers by electrospinning method and the oxygen quenching fluorescence behavior was systematically investigated. The linear Stern-Volmer model, the Demas and Lehrer models were used to fit the obtained Stern-Volmer curves of the composite fibers. An oxygen sensor based on the D-Re(I) composite fibers shows short response time, good reproducible signals, and linear Stern-Volmer plots attributed to the existence of the ligand containing long alkyl chain groups that makes D-Re(I) become soluble in the polymers.

**Key words**: oxygen sensing; electrospinning fiber; dirhenium(Ⅰ) complex

# 双核铼配合物复合电纺纤维的制备和氧传感性能的研究

刘艳红[1,2], 李 斌[1], 丛 妍[1,2]

(1. 中国科学院 长春光学精密机械与物理研究所 激发态物理重点实验室, 吉林 长春 130033;
2. 中国科学院 研究生院, 北京 100039)

**摘要**: 合成了亲脂性双核铼配合物 *fac*-[{Re(CO)$_3$(d19-phen)}$_2$(4,4′-bipyridylacetylene)](OTf)$_2$, 将此配合物均匀地分散到聚苯乙烯(PS)和聚甲基丙烯酸甲酯(PMMA)中, 通过电纺方法, 得到复合材料纤维, 并系统地研究了它们的氧传感性能。分别用线性 Stern-Volmer 模型, Demas 双格位模型以及 Lehrer 模型对所得到的 Stern-Volmer 曲线进行了拟合, 实验结果表明, 这种复合纤维氧传感材料显示了短的响应时间, 可逆的氧传感信号, 而且由于含有亲脂性的长链烷烃配体的存在, 使得铼配合物在聚合物中分散均匀, 从而得到线性关系较好的 Stern-Volmer 曲线。

**关 键 词**: 氧传感; 电纺纤维; 双核铼(Ⅰ)配合物
**中图分类号**: TB34 **文献标识码**: A

**收稿日期**: 2008-08-11; **修订日期**: 2008-10-18.
Foundation item: supported by the National Natural Science Foundations of China (No. 50872130).

## 1 Introduction

Quantitative determination of oxygen concentration is important in chemical analysis related to environmental, clinical and industrial applications[1-3]. Compared with the traditional amperometry using oxygen electrodes, which are limited by the stability of the electrode surface and instabilities in the oxygen diffusion barrier, optical oxygen sensors based on luminescence quenching by oxygen on the intensity($I$) or excited state lifetime($\tau$) of a luminophore(fluorophore or phosphore) are the popular alternative because of no oxygen consumption, no requirement for a reference electrode, inertness against sample flow rate or stirring speed and immunity to exterior electromagnetic field interference. In the fabrication of an oxygen sensing material, the indicator dye has to be immobilized in oxygen permeable matrix such as silica sol-gel thin films[4], poly(dimethylsiloxane)(PDMS)[5], polystyrene(PS)[6], polymethylmethacrylate(PMMA)[7] and mesoporous molecular sieve[8].

The most commonly used indicator dyes are transition metal complexes. Luminescent Ru(Ⅱ) diimine complexes[8], exhibiting high quantum yields and relatively long luminescent lifetimes and oxygen-sensitivity, predominate among the optical oxygen sensors. Pd and Pt porphyrins[9] complexes exhibiting emission lifetimes in the millisecond range have also been proved to be excellently suitable for oxygen sensing.

Re(Ⅰ) complexes were used as phosphorescent emitters in organic light emitting device(OLED) applications and potential biological probes in bioinorganic chemistry with promising properties of high quantum yields($\Phi = 0.4 \sim 0.7$)[10]. However, to our knowledge, Re(Ⅰ) complex has rarely been reported as an oxygen sensor probe[11,12]. For the transition metal complexes, properties including the quantum yields, $\tau$ values, charges, shapes, and site selective binding can be systematically tailored by modifying the ligands or metal ions. The lipophilicity generally improves the solubility of the organometallic complexes in hydrophobic polymers such as PS and PMMA used for chemical sensing.

Electrospinning is a novel and cost-effective technique for fabricating one-dimensional (1D) nano- or microfibers for a variety of applications, including sensors[13]. It consists of a spinneret with a conductive capillary, a high-voltage power supply, and a collector. Spinning solution is loaded into the capillary to form a droplet at the tip. When a voltage applied to the conductive capillary overcomes the surface tension forces, the droplet is first stretched into a cone called a "Taylor cone" and finally into an electrified jet then moves toward the collector with diameters from a few micrometers to nanometers.

In this study, the ligand 4,7-dinonadecyl-1,10-phenanthroline(d19-phen) containing long alkyl chain groups was synthesized and the corresponding lipophilic dirhenium(Ⅰ) complex D-Re(Ⅰ) was prepared. The oxygen sensing properties of D-Re(Ⅰ)/PS and D-Re(Ⅰ)/PMMA electrospinning fibers were systematically evaluated.

## 2 Experimental section

### 2.1 Reagents and measurement

Both polystyrene($M_w \approx 250\ 000$) and polymethylmethacrylate($M_w \approx 350\ 000$) were obtained commercially from Sigma-Aldrich. Analytical grade solvents and compounds were used for preparations without further purification.

The morphology of products was observed by Hitachi-4800 scanning electron microscope(SEM). $^1$H NMR spectra were recorded on a Bruker AC 400 spectrometer. The oxygen sensing properties based on luminescence intensity quenching of the composite fibers were characterized using a Hitachi-4500 fluorescence spectrophotometer equipped with a

xenon lamp(150 W) operating in the range of 200 ~ 900 nm. For the Stern-Volmer plot measurements, oxygen and nitrogen were mixed at different concentrations via gas-flow controllers and flowed directly into the gas chamber sealed with a close fitting suba-seal rubber lid equipped with two (in and out) tubes. 1 min is usually allowed between changes of the $N_2/O_2$ concentrations to ensure that a new equilibrium point had been established. Equilibrium was evident when the luminescence intensity remained constant(±2%). The sensing response curves were obtained using the same instruments.

## 2.2 Synthesis of the D-Re(Ⅰ) complex

Figure 1 shows the molecular structure of D-Re(Ⅰ). The ligand 4,7-dinonadecyl-1,10-phenanthroline (d19-phen) was obtained according to the literature[14]. The D-Re(Ⅰ) was synthesized by modification of reported literatures[15]: 0.3 mmol $Re(CO)_5Cl$ and 0.3 mmol d19-phen were dissolved in 16 mL benzene and refluxed for 2 h under $N_2$ flow and fac-$ClRe(CO)_3$(d19-phen) was obtained by evaporating the solvent and subsequent recrystallization from dichloromethane/hexane. Then 0.2 mmol *fac*-$ClRe(CO)_3$(d19-phen) and 0.3 mmol silver trifluoromethanesulfonate (AgOTf) were mixed and refluxed in acetonitile for 8 h in the dark under $N_2$, from which a white residue with a clear yellow solution was obtained. After filtration, the filtrate was evaporated to give a bright yellow solid *fac*-[$(CH_3CN)Re(CO)_3$(d19-phen)]OTf (Re(Ⅰ)). Finally, 0.1 mmol Re(Ⅰ) and 0.05 mmol bridging ligand 4,4′-bipyridyl were refluxed in benzene for 24 h under $N_2$. The resulting solution was evaporated to give a bright yellow residue, which was purified by column chromatography (silica-gel using ethyl acetate/*n*-hexane (1∶1, *v*/*v*) as the eluent). The desired dirhenium(Ⅰ) complex was finally obtained. Yield: 32%. $^1H$ NMR (300 MHz, $CDCl_3$, relative to $Me_4Si$): $\delta$ d19-phen: 3.31 (m, 4H, $-CH_2-$), 3.19 (m, 4H, $-CH_2-$), 1.82 (m, 8H, $-CH_2-$), 1.49 (m, 8H, $-CH_2-$), 1.26 (m, 120H, $-(CH_2)_{15}-$), 0.88 (t, 12H, $J$ = 6.6 Hz, $-CH_3$), 9.36 (d, 4H, $J$ = 5.5 Hz, H at 2,9-position), 8.17 (s, 4H, H at 5,6-position), 7.88 (d, 4H, $J$ = 5.4 Hz, H at 3,8-position), 4,4′-bipyridyl: 8.28 (d, 4H, $J$ = 6.7 Hz, ortho to N), 6.68 (d, 4H, $J$ = 6.8 Hz, meta to N).

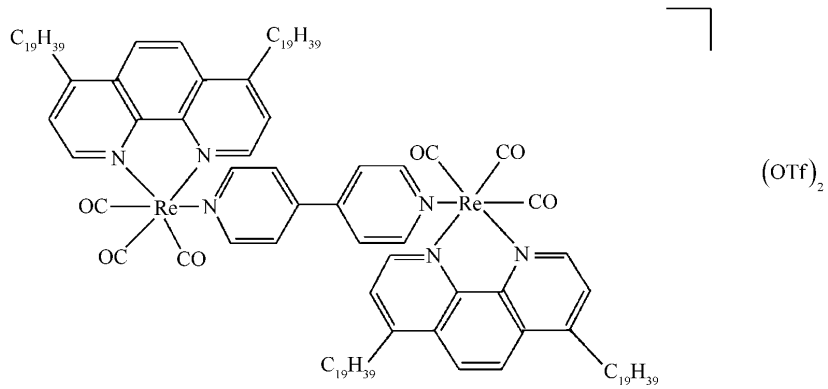


Fig. 1　Molecular structure of complex D-Re(Ⅰ)

## 2.3 Preparation of the composite fibers

0.001 g D-Re(Ⅰ) was dissolved in dimethylformamide solutions of PMMA (0.12 g/mL) and PS (0.3 g/mL), respectively. The solutions were freshly prepared and stirred thoroughly for 24 h before electrospinning. For PS, 1% (CTAB) relative to PS was added under vigorous stirring to prepare uniform fibers by electrospinning. In the electrospinning of composite fibers, the voltage used was 18 kV and the distance between the spinneret and collector plate was held at 25 cm. The as obtained composite fibers are denoted as D-Re(Ⅰ)/

PS and D-Re(Ⅰ)/PMMA, respectively.

## 3 Results and discussion

Figure 2 shows the SEM images of the D-Re(Ⅰ)/PS (Fig. 2(a)) and D-Re(Ⅰ)/PMMA (Fig. 2(b)) composite fibers. It can be seen that uniform fibers were formed for both of the composite samples. The average diameters were 1.5 μm and 2 μm for D-Re(Ⅰ)/PS and D-Re(Ⅰ)/PMMA, respectively.

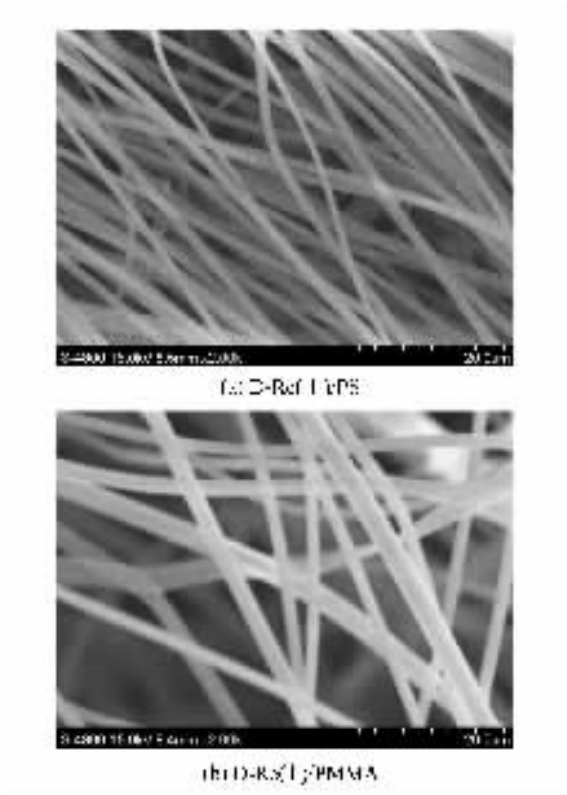

Fig. 2 Typical SEM images of composite fibers

Figure 3 shows the room temperature fluorescence emission spectra of D-Re(Ⅰ)/PS (Fig. 3(a)) and D-Re(Ⅰ)/PMMA (Fig. 3(b)) composite fibers at different oxygen concentrations. Excitation of the samples at $\lambda = 400$ nm produces intense, broad and featureless emissions. The emission peaks were observed at 543 and 522 nm respectively, which arise from ligand to metal charge-transfer excited state. It can be seen that the relative emission intensity decreased as the oxygen volume fraction increased and the emission peak showed no shift.

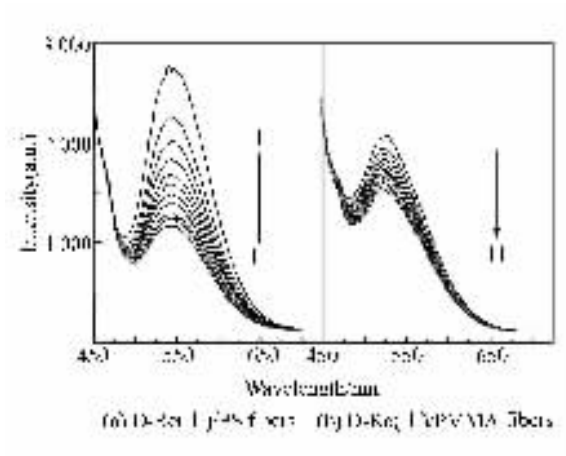

Fig. 3 Emission spectra of D-Re(Ⅰ)/PS fibers (a) and D-Re(Ⅰ)/PMMA fibers (b) measured at different oxygen volume fractions (1) 0 V%; (2) 10 V%; (3) 20 V%; (4) 30 V%; (5) 40 V%; (6) 50 V%; (7) 60 V%; (8) 70 V%; (9) 80 V%; (10) 90 V%; (11) 100 V%.

Figure 4 presents the typical intensity-based Stern-Volmer plots for D-Re(Ⅰ)/PS and D-Re(Ⅰ)/PMMA composite fibers. The solid lines represent the best fits to the data.

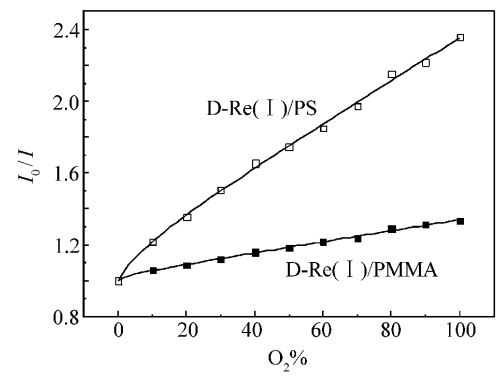


Fig. 4 Typical Stern-Volmer plots of D-Re(Ⅰ)/PS and D-Re(Ⅰ)/PMMA fibers.
The solid lines represent the best fit using the two-site Demas model.

Optical sensors based on the luminescence quenching are examined by the Stern-Volmer equation. In homogeneous media with only a single-component exponential decay, the intensity and life-

time form of the Stern-Volmer equation[8] is

$$I_0/I = \tau_0/\tau = 1 + K_{sv}[O_2], \quad (1)$$

where $[O_2]$ is the oxygen concentration, $\tau_0$ and $\tau$ are lifetimes, $I_0$ and $I$ are intensities. The subscript 0 denotes the value in the absence of quencher. $K_{sv}$ is the Stern – Volmer constant.

However, the nonlinear Stern-Volmer equation is often the case, in which Demas two-site model could have excellent ability to fit the experiment data. In this model, the straight-line intensity Stern-Volmer equation[16] then becomes

$$\frac{I_0}{I} = \frac{1}{f_{01}/(1 + K_{sv1}P_{O_2}) + f_{02}/(1 + K_{sv2}P_{O_2})}, \quad (2)$$

where $f_{0i}$ values are the fraction of each of the two sites contributing to the unquenched intensity, $P_{O_2}$ is the partial pressure of oxygen at 1 atmosphere pressure, and $K_{svi}$ values are the associated Stern-Volmer quenching constants for the two sites, one of which is easily be quenched but the other is not. Meanwhile, when $K_{sv2} = 0$, the Demas model collapses to Lehrer model[17], which is also able to fit the experiment data reasonably. The equation is shown below.

$$\frac{I_0}{I} = \frac{1}{f_{01}/(1 + K_{sv1}P_{O_2}) + f_{02}}, \quad (3)$$

The D-Re(Ⅰ)/PS and D-Re(Ⅰ)/PMMA composite fibers show excellent linearity of oxygen quenching plots. This may be due to that the existence of the long alkyl chain in d19-phen that improved the solubility of D-Re(Ⅰ) in the polymers. Linear calibration Stern-Volmer plot of oxygen sensor is very important because it is easy to calibrate and does not require a multipoint calibration strategy when exposed to practical applications. As shown in Figure 4, the Stern-Volmer oxygen quenching plots of D-Re(Ⅰ)/PS and D-Re(Ⅰ)/PMMA composite fibers appear to deviate from single exponential to just a small extent especially at low $O_2$ concentration. The downward curvature plots necessitate a more complex model than a single species quenched bimolecularly. The Demas two-site model is enough to fit the intensity-quenching curves of all these samples. It is not surprising given the well-known ability of two exponentials to give excellent fits to complex decay curves, which are made up of distribution function of exponential decays, especially at the count levels used on most single-photo-counting instruments[8]. The intensity-based linear Stern-Volmer, Demas two-site model and Lehrer model oxygen quenching fitting parameters are also tabulated in Table 1.

**Table 1 Intensity-based Stern-Volmer oxygen quenching parameters of the composite fibers from fitting different models, Linear Stern-Volmer Model, Lehrer Model and Demas Two-site Model**

| | | D-Re(Ⅰ)/PMMA | D-Re(Ⅰ)/PS |
|---|---|---|---|
| Linear Stern-Volmer | $K_{sv}$ | 0.003 53 | 0.014 14 |
| | $r^2$ | 0.982 48 | 0.982 48 |
| Demas | $K_{sv1}$ | 0.002 96 | 0.009 76 |
| | $K_{sv2}$ | 0.320 83 | 0.134 65 |
| | $f_{01}$ | 0.965 63 | 0.814 19 |
| | $r^2$ | 0.997 46 | 0.997 92 |
| Lehrer | $K_{sv1}$ | 0.007 76 | 0.021 55 |
| | $f_{01}$ | 0.572 44 | 0.835 83 |
| | $r^2$ | 0.994 74 | 0.995 22 |

Figure 5 shows the typical dynamic response of samples on exposures to pure $N_2$ and $O_2$ atmosphere, which were varied periodically. From this time dependent measurements, the 95% response ($t_{95\downarrow}$) and 95% recovery ($t_{95\uparrow}$) time to an alternating atmosphere of pure $N_2$ and $O_2$ can be calculated. These values are defined as the time taken for a sample to attain 95% of its total emission intensity change when the gas is changed from pure $N_2$ to pure $O_2$ and from pure $O_2$ to pure $N_2$, respectively. D-Re(Ⅰ)/PS and D-Re(Ⅰ)/PMMA composite fibers exhibit a fully reversible response and recovery with $t_{95\downarrow}$ = 15 s, 11 s and $t_{95\uparrow}$ = 30 s, 27 s, respectively. This result shows that the recovery time is longer than the response time, and this obvious difference

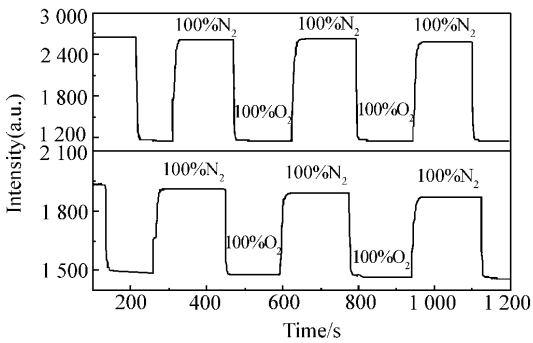


Fig. 5 Quenching responses and relative emission changes vs time of D-Re(Ⅰ)/PMMA(bottom) and D-Re(Ⅰ)/PS(top) oxygen sensing materials on periodically cycling from 100% nitrogen to 100% oxygen atmosphere.

can be explained by the mathematical expressions developed by Mills et al. to describe the diffusion-controlled dynamic response and recovery behavior of a hyperbolic-type sensor to changing analyte concentration[18]. It is well known that the reproducibility of oxygen sensing materials under irradiation is one of the key analytical characters of merit for practical application. Inspection of these results in Figure 5 reveals that stable and reproducible signals upon repeated exposure to oxygen/nitrogen cycles are obtained for both of the D-Re(Ⅰ)/PS and D-Re(Ⅰ)/PMMA composite fibers.

## 4 Conclusion

In this study, the lipophilic dirhenium complex D-Re(Ⅰ) was synthesized and homogenously doped into PS and PMMA, respectively. Both of D-Re(Ⅰ)/PS and D-Re(Ⅰ)/PMMA electrospinning fibers were optically sensitive to oxygen and the oxygen sensing properties were systematically investigated. The composite fibers show linear Stern-Volmer plots, short response time and good reproducible signals as an oxygen sensor.

References:

[1] PREININGER C, KLIMANT I, WOLFBEIS O S. Optical fiber sensor for biological oxygen demand[J]. *Anal. Chem.*, 1994, 66(11): 1841-1846.

[2] MITSUBAYASHI K, WAKABAYASHI Y, MUROTOMI D, *et al.*. Wearable and flexible oxygen sensor for transcutaneous oxygen monitoring[J]. *Sens. Actuators B*, 2003, 95(1-3): 373-377.

[3] WHIFFIN V S, COONEY M J, CORD-RUWISCH R. Online detection of feed demand in high cell density cultures of Escherichia coli by measurement of changes in dissolved oxygen transients in complex[J]. *Biotechnol. Bioeng.*, 2004, 85(4): 422-433.

[4] BUKOWSKI R M, CIRIMINNA R, BRIGHT F V, *et al.*. High-performance quenchometric oxygen sensors based on fluorinated xerogels doped with $[Ru(dpp)_3]^{2+}$[J]. *Anal. Chem.*, 2005, 77(8): 2670-2672.

[5] MARIA C D, PETER J M, ROBERT J C, *et al.*. Synthesis, characterization, and evaluation of $[Ir(ppy)_2(vpy)Cl]$ as a polymer-bound oxygen sensor[J]. *Inorg. Chem.*, 2003, 42(16): 4864-4872.

[6] HARTMAN P, TRETTNAK W. Effects of polymer matrices on calibration functions of luminescent oxygen sensors based on porphyrin ketone complexes[J]. *Anal. Chem.*, 1996, 68(15): 2615-2620.

[7] DOUGLAS P, EATON K. Response characteristics of thin film oxygen sensors. Pt and Pd octaethylporphyrins in polymer films[J]. *Sens. Actuators B.*, 2002, 82(2-3): 200-208.

[8] LEI B F, LI B, ZHANG H R, *et al.*. Mesostructured silica chemically doped with Ru(II) as superior optical oxygen sensor[J]. *Adv. Funct. Mater.*, 2006, 16(14): 1883-1891.

[9] ZHANG H, SUN Y, WANG Y, *et al.*. Oxygen sensing materials based on mesoporous silica MCM-41 and Pt(II)-porphyrin complexes[J]. *J. Mater. Chem.*, 2005, 15 3181-3196.

[10] SACKSTEDER L, DEMAS J N, DEGRAFF B A, *et al.*. Long-lived highly luminescent rhenium(I) complexes as molecular probes: intra- and intermolecular excited-state interactions[J]. *J. Am. Chem. Soc.*, 1993, 115(18): 8230-8238.

[11] LOAN H, ZHUO W, MITCHELL A W, *et al*.. Evaluation of phosphorescent rhenium and iridium complexes in polythionylphosphazene films for oxgen sensor applications[J]. *Chem. Mater.*, 2005, 17(19): 4765-4773.

[12] SACKSTEDER L A, DEMAS J N, DEGRAFF B A. Design of oxygen sensors based on quenching of luminescent metal complexes: effect of ligand size on heterogeneity[J]. *Anal. Chem.*, 1993, 65(23): 3480-3483.

[13] RENEKER D H, CHUN I. Nanometre diameter fibres of polymer produced by electrospinning[J]. *Nanotechnology*, 1996, 7: 216-223.

[14] KATRITZKY A R, LONG Q H, MALHOTRA N, *et al*.. Synthesis of 4.7-substituted 1.10-phenanthrolines[J]. *Synthesis*, 1992, 10: 911-913.

[15] SULLIVAN B P, MEYER T J. Photoinduced irreversible insertion of $CO_2$ into a metal-hydride bond[J]. *J. Chem. Soc. Chem. Commun.*, 1984, 18: 1244-1245.

[16] TANG Y, TEHAN E C, BRIGHT F V, *et al*.. Sol-gel-derived sensor materials that yield linear calibration plots high sensitivity and long-term stability[J]. *Anal. Chem.*, 2003, 75(10): 2407-2413.

[17] LEHRER S S. Solute perturbation of protein fluorescence quenching of the tryptophyl fluorescence of model compounds and of lysozyme by iodide ion[J]. *Biochemistry*, 1970, 10(17): 3254-3263.

[18] MILLS A, CHANG Q. Modelled diffusion-controlled response and recovery behaviour of a naked optical film sensor with a hyperbolic-type response to analyte concentration[J]. *Analyst*, 1992, 117: 1461-1466.

**作者简介**：**刘艳红**(1981—)，**女，黑龙江大庆人，博士研究生，主要从事有机及无机发光材料的研究。**E-mail: liuyanh123@126.com

**李　斌**(1964—)，**男，研究员，博士生导师，主要从事有机及无机发光材料的研究。**E-mail: lib020@ciomp.ac.cn